Available online at www.sciencedirect.com
SCIENCE DIRECT®
Bioorganic & Medicinal Chemistry 13 (2005) 6188–6194
Bioorganic & Medicinal Chemistry

Synthesis and in vivo evaluation of a novel peripheral benzodiazepine receptor PET radioligand

Michelle L. James,[a] Roger R. Fulton,[b,c] David J. Henderson,[b] Stefan Eberl,[b] Steven R. Meikle,[b] Sally Thomson,[d] Robin D. Allan,[a] Frederic Dolle,[e] Michael J. Fulham[b,f] and Michael Kassiou[a,b,*]

[a]*Department of Pharmacology, University of Sydney, NSW 2006, Australia*
[b]*Department of PET and Nuclear Medicine, Royal Prince Alfred Hospital, Missenden Road, Camperdown, NSW 2050, Australia*
[c]*School of Physics, University of Sydney, NSW 2006, Australia*
[d]*Department of Renal Medicine, Royal Prince Alfred Hospital, Missenden Road, Camperdown, NSW 2050, Australia*
[e]*Service Hospitalier Frédéric Joliot, Département de Recherche Médicale, CEA/DSV, 4 Place du Général Leclerc, F-91401 Orsay, France*
[f]*Faculty of Medicine, University of Sydney, NSW 2006, Australia*

Received 31 May 2005; revised 16 June 2005; accepted 17 June 2005
Available online 20 July 2005

Abstract—The novel pyrazolopyrimidine ligand, *N*,*N*-diethyl-2-[2-(4-methoxyphenyl)-5,7-dimethyl-pyrazolo[1,5-*a*]pyrimidin-3-yl]-acetamide **1** (DPA-713), has been reported as a potent ligand for the peripheral benzodiazepine receptor (PBR) displaying an affinity of K_i = 4.7 nM. In this study, **1** was successfully synthesised and demethylated to form the phenolic derivative **6** as precursor for labelling with carbon-11 ($t_{1/2}$ = 20.4 min). [^{11}C]**1** was prepared by O-alkylation of **6** with [^{11}C]methyl iodide. The radiochemical yield of [^{11}C]**1** was 9% (non-decay corrected) with a specific activity of 36 GBq/μmol at the end of synthesis. The average time of synthesis including formulation was 13.2 min with a radiochemical purity >98%. In vivo assessment of [^{11}C]**1** was performed in a healthy *Papio hamadryas* baboon using positron emission tomography (PET). Following iv administration of [^{11}C]**1**, significant accumulation was observed in the baboon brain and peripheral organs. In the brain, the radioactivity peaked at 20 min and remained constant for the duration of the imaging experiment. Pre-treatment with the PBR-specific ligand, PK 11195 (5 mg/kg), effectively reduced the binding of [^{11}C]**1** at 60 min by 70% in the whole brain, whereas pre-treatment with the central benzodiazepine receptor ligand, flumazenil (1 mg/kg), had no inhibitory effect on [^{11}C]**1** uptake. These results indicate that accumulation of [^{11}C]**1** in the baboon represents selective binding to the PBR. These exceptional in vivo binding properties suggest that [^{11}C]**1** may be useful for imaging the PBR in disease states. Furthermore, [^{11}C]**1** represents the first ligand of its pharmacological class to be labelled for PET studies and therefore has the potential to generate new information on the pathological role of the PBR in vivo.

1. Introduction

The peripheral benzodiazepine receptor (PBR) was originally characterised as an alternative binding site for the benzodiazepine, diazepam,[1] and was thought to be a subtype of the central benzodiazepine receptor (CBR). Later studies identified the PBR to be a separate class of receptor due to its distinct structure, physiological functions and subcellular location on the outer membrane of the mitochondria.[2] Currently, it is understood that the PBR forms a trimeric complex with the adenine nucleotide carrier (ANC) (30 kDa) and the voltage-dependent anion channel (VDAC) (32 kDa) to constitute the mitochondrial permeability transition pore (MPTP).[2] Although the PBR has been implicated in numerous biological processes, its exact physiological role remains unclear. Studies implicate the importance of the PBR in the rate-limiting step of steroid biosynthesis,[3] immunomodulation,[4] porphyrin transport,[5] calcium homeostasis and programmed cell death.[6]

The PBR is densely distributed in most peripheral organs including the lungs, heart and kidneys, yet it is only minimally expressed in the normal brain parenchyma.[7]

Keywords: Pyrazolopyrimidine; Peripheral benzodiazepine receptor; Carbon-11; PET.
* Corresponding author. Tel.: +612 9515 5150; fax: +612 9515 6381; e-mail: mkassiou@med.usyd.edu.au

0968-0896/$ - see front matter © 2005 Elsevier Ltd. All rights reserved.
doi:10.1016/j.bmc.2005.06.030

Following neuronal injury, PBR expression is dramatically increased.[8] In vivo studies in patients suffering from Alzheimer's disease (AD) and multiple sclerosis (MS) confirmed that elevation of PBR binding is primarily localised on activated microglial cells.[9] Microglia, the resident macrophages of the CNS, are extremely sensitive to alterations to their microenvironment and hence readily become activated due to injury or infection.[10] For this reason, the PBR are believed to be intimately associated with initial inflammatory processes in the early stages of several neurological diseases.[11] However, the exact role of microglia in the pathology of these diseases has not been completely elucidated due to the lack of specific and selective PBR ligands.

The development of novel PBR radioligands for non-invasive imaging with positron emission tomography (PET) has enabled study of microglial activation in the living brain. The isoquinoline carboxamide [^{11}C](*R*)-PK 11195 has been extensively used as a pharmacological probe for studying the function and expression of PBRs.[12] A number of PET studies conducted in patients with AD,[13] MS[14] and multiple system atrophy (MSA)[15] have shown that measurement of PBRs in vivo with [^{11}C](*R*)-PK 11195 is feasible in the living brain. However, [^{11}C](*R*)-PK 11195 displays a poor signal-to-noise ratio and has demonstrated low brain permeability which ultimately decreases its sensitivity in detecting areas of microglial activation. These unfavourable characteristics may be attributable to the tracer's high lipophilicity and low bioavailability (88% bound to plasma protein).[7]

The development of PBR ligands with improved brain kinetics is vital to understand the cellular processes underlying numerous disease states. Selective and specific PBR ligands may also have the potential to serve as diagnostic and therapeutic tools. The recently synthesised [^{11}C]DAA1106 has demonstrated a high specificity for the PBR in rodent[16] and primate brains[17] and is an attractive candidate for PET imaging of the PBR in humans.

Another class of PBR ligands, the pyrazolopyrimidines, have been reported and although displaying high affinity are yet to be radiolabelled for use in PET. One of the lead compounds from this series, **1** (DPA-713) (shown in Scheme 1), has a higher affinity (K_i = 4.7 nM) for the PBR than PK 11195 (K_i = 9.3 nM) and is notably more selective for the PBR over the CBR (K_i > 10,000 nM for CBR).[18] The aim of the present study was to label **1** (DPA-713) with carbon-11 and perform preliminary in vivo assessment in a healthy baboon using PET.

2. Results and discussion

2.1. Chemistry

N,*N*-Diethyl-2-[2-(4-methoxy-phenyl)-5,7-dimethylpyrazolo[1,5-*a*]pyrimidin-3-yl]-acetamide (**1**, as reference) was synthesised in four chemical steps with some modifications to literature procedures[18–20] (Scheme 1).

The aroylacetonitrile, **3**, was formed in 17% yield by reaction of commercially available methyl-4-methoxy

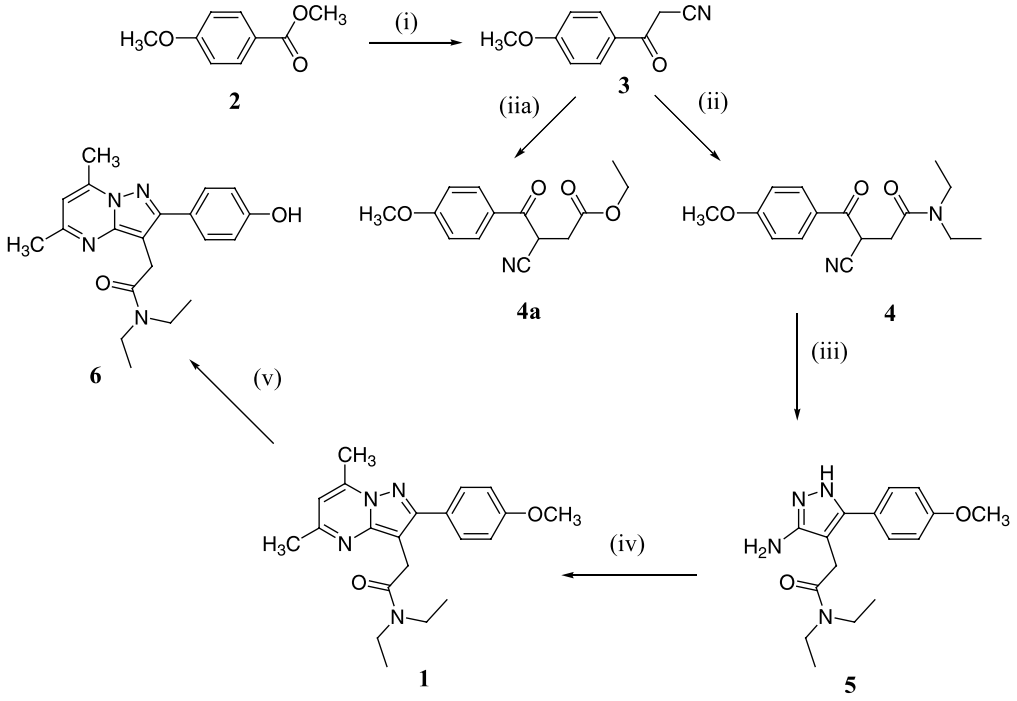

Scheme 1. Reagents and conditions: Synthesis of *N*,*N*-diethyl-2-[2-(4-methoxy-phenyl)-5,7-dimethylpyrazolo[1,5-*a*]pyrimidin-3-yl]-acetamide (**1**) (DPA-713) and the radiolabelling precursor *N*,*N*-diethyl-2-[2-(4-hydroxy-phenyl)-5,7-dimethyl-pyrazolo[1,5-*a*]pyrimidin-3-yl]-acetamide (**6**); (i) acetonitrile, sodium methoxide, 100 °C, 24 h; (iia) *N*,*N*-diethylchloroacetamide, sodium iodide, NaOH/80% EtOH, reflux 7 h; (ii) *N*,*N*-diethylchloroacetamide, sodium iodide, NaOH/80% EtOH, rt, 7 h; (iii) hydrazine hydrate, EtOH, acetic acid, reflux 4 h; (iv) 2,4-pentadione, EtOH, reflux 12 h; (v) 48% HBr, tributylhexadecylphosphonium bromide, 100 °C, 7 h.

benzoate **2** with acetonitrile in the presence of sodium methoxide at 100 °C. Rearrangement of purification steps reported in the literature allowed the benzoic acid (structure not shown) by-product to be removed more efficiently leading to improved purity and yield of the final product. The reactivity of the methylene group in **3** was exploited by reacting it in an alkaline solution with *N*,*N*-diethylchloroacetamide and sodium iodide. However, the product (**4a**) isolated after 7 h reflux displayed ^{1}H NMR and mass spectrum indicative of an ethyl ester functional group instead of the desired diethyl amide moiety. Repeating the same reaction under milder conditions at room temperature afforded **4** in 64% yield as confirmed by ^{1}H NMR and mass spectrum. In the third step, **4** was converted to the pyrazole **5** by heating at reflux in ethanol with hydrazine hydrate, in the presence of acetic acid. The condensation of **5** with the electrophilic reagent, 2,4-pentadione, led to closure of the pyrimidine ring to yield the title compound **1** as pale yellow crystals in 93% yield. Compound **1** was subsequently demethylated by heating in a solution of hexadecyl tributyl phosphonium bromide in 45% HBr to form the phenolic derivative **6** (*N*,*N*-diethyl-2-[2-(4-hydroxyphenyl)-5,7-dimethyl-pyrazolo[1,5-*a*]pyrimidin-3-yl]-acetamide), as precursor for labelling with carbon-11 in 54% yield.

2.2. Radiochemistry

The pyrazolopyrimidine **1** was labelled with carbon-11 ($t_{1/2}$ = 20.4 min) using [^{11}C]methyl iodide ([^{11}C]CH_3I) and the phenolic precursor **6** (Scheme 2).

[^{11}C]CH_3I was synthesised from cyclotron-produced [^{11}C]carbon dioxide ([^{11}C]CO_2), trapped in a DMF solution containing **6** and tetrabutyl ammonium hydroxide (TBAH) and allowed to react at room temperature for 3 min. The reaction mixture was purified via reverse-phase semi-preparative high-performance liquid chromatography (HPLC). This afforded [^{11}C]**1** in 9% (n = 6) non-decay corrected radiochemical yield based on starting [^{11}C]CH_3I in an average synthesis time of 13.2 min (including HPLC purification and formulation). Co-injection of the non-radioactive **1** was performed using analytical HPLC to confirm the identity of the product. In the final product solution, radiochemical and chemical purity was greater than 98% with a specific activity of 36 GBq/μmol. No attempts were made to optimise these conditions as sufficient quantities of the radioligand were produced to enable pharmacological evaluation.

Formulation of labelled product for iv injection was achieved by: (1) evaporation of HPLC solvent; (2) reconstitution of residue in physiological saline (2 mL) and (3) sterile filtration through a 0.22 μm filter. The final injectable solution was clear and colourless with a pH of 5.0. The preparation was free from starting labelling precursor. Administration to the animal was performed within 10 min following end of synthesis in each study.

2.3. Pharmacology

2.3.1. Evaluation using PET. The uptake of [^{11}C]**1** was examined using PET. Dynamic PET brain imaging commenced just prior to iv administration of [^{11}C]**1** (200 MBq in 2 mL saline) and was terminated 60 min post-injection. This was immediately followed by a whole body acquisition for 2 min at each of six bed positions. Figure 1a shows a 60-min PET summation image of a 3.4 mm thick transaxial baboon brain slice from the dynamic scan. The PET image provided visual evidence for the ability of [^{11}C]**1** to traverse the blood–brain barrier (BBB) with considerable accumulation of radioactivity in the baboon brain.

The whole brain uptake of [^{11}C]**1** as a function of time is represented graphically in Figure 2. [^{11}C]**1** reached maximal uptake after 20 min and stayed at approximately the same uptake level for the remaining 40 min of imaging.

In an earlier reported study using *Papio anubis* baboons, time–activity curves (TACs) of [^{11}C](*R*)-PK 11195 brain uptake provided evidence of rapid BBB penetration and maximal brain activity within 3–5 min.[21] Directly following maximum brain uptake, [^{11}C](*R*)-PK 11195 activity steeply declined to the plasma level. This dramatic washout of [^{11}C](*R*)-PK 11195 between 15 and 20 min was later revealed to be a consequence of binding to plasma proteins.[22] Because the uptake of [^{11}C](*R*)-PK 11195 closely resembled that of blood flow, PET images generated were not indicative of specific binding to the PBR. In contrast, the slower kinetics of [^{11}C]**1** enabled longer imaging in which signals at later time points were attributable to specific PBR binding. For this reason, [^{11}C]**1** may provide a more accurate assessment of PBR density than the widely used [^{11}C](*R*)-PK 11195.

2.3.2. Blocking studies. The in vivo specificity and selectivity of [^{11}C]**1** in the baboon brain was assessed via two blocking studies which were performed 3 weeks apart:

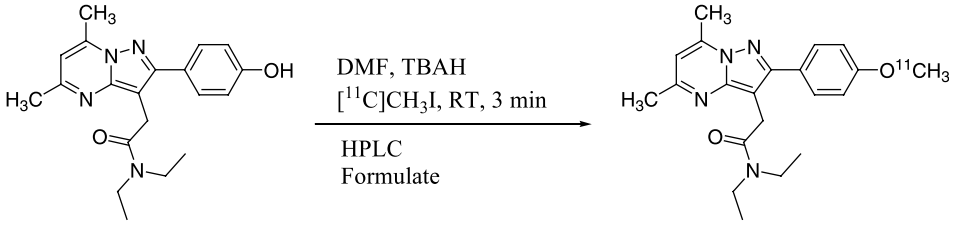

6 [^{11}C]**1**

Scheme 2. Radiosynthesis of *N*,*N*-diethyl-2-[2-(4-[^{11}C]methoxy-phenyl)-5,7-dimethyl-pyrazolo[1,5-*a*]pyrimidin-3-yl]-acetamide, ([^{11}C]**1**).

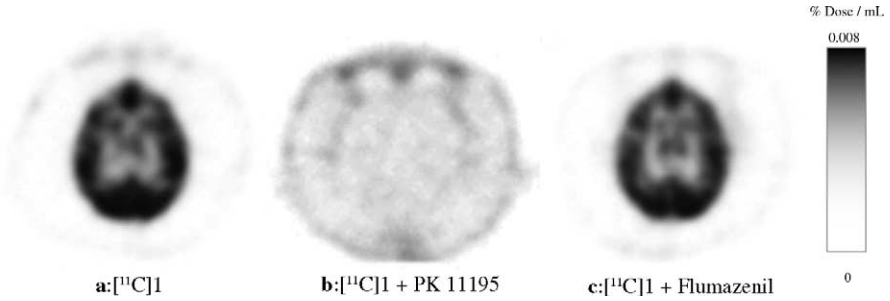

Figure 1. PET summation images of a single transaxial brain slice over 60 min: (a) [^{11}C]**1**, (b) [^{11}C]**1** + PK 11195 (5 mg/kg) and (c) [^{11}C]**1** + flumazenil (1 mg/kg). Images (a) and (c) are slightly over saturated to allow visualization of image (b).

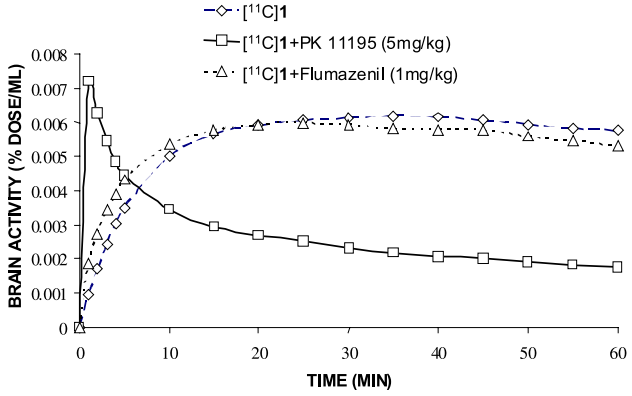

Figure 2. Whole brain TACs in baseline study with [^{11}C]**1** and blocking studies performed with PK 11195 and flumazenil.

one using the PBR-specific ligand, PK 11195, and the other using the CBR-specific ligand, flumazenil. Pre-treatment of the baboon with PK 11195 (5 mg/kg, iv, 5 min prior to radioligand injection) resulted in markedly decreased uptake of [^{11}C]**1** (Fig. 1b) compared to the baseline study (Fig. 1a). In contrast, pre-treatment with flumazenil (1 mg/kg, iv, 5 min prior to radioligand injection) displayed no inhibitory effect on [^{11}C]**1** uptake (Fig. 1c). These results clearly demonstrated that retention of [^{11}C]**1** in the baboon brain represents selective binding to the PBR and not the CBR.

The TACs (Fig. 2) for the baseline study and pharmacological challenge with flumazenil in the whole brain were similar, indicating no inhibitory effect on [^{11}C]**1** uptake. These results compare well to those generated in studies with the PBR-specific ligand [^{11}C]DAA1106 and 0.1 mg/kg flumazenil.[17] Pharmacological challenge using PK 11195 resulted in TACs symptomatic of radioligand inhibition. Consequently, [^{11}C]**1** was washed out of the brain within 10 min, denoted by the rapid decline in the TAC. Similar results have been reported for PK 11195 blocking studies with both [^{11}C]DAA1106[17] and [^{11}C](*R*)-PK 11195.[21]

Figure 3a–c show the whole body images of the baboon, which were acquired at the conclusion of dynamic scanning in all three studies. These images demonstrate the significant inhibition of [^{11}C]**1** uptake in the brain, heart and kidneys following pre-treatment with PK 11195, thus providing evidence that [^{11}C]**1** was specifically bound to the PBR in peripheral organs. No inhibitory effects were observed in the flumazenil blocking study, which indicated the selectivity of [^{11}C]**1** for the PBR over the CBR in peripheral organs.

Log *P* values for **1** and PK 11195 using HPLC analysis were found to be 2.4 and 3.4, respectively. It is recommended that the log of the octanol–water partition coefficient (log *P*) for CNS radioligands be between 2 and 3 in order to achieve a high brain uptake relative to weak non-specific binding.[23] The log *P* of compound **1** is thus within the optimum range which is supported by its rapid penetration of the BBB and high specific binding to the PBR. Compound **1** is clearly less lipophilic than PK 11195 which may partly explain the different degrees of specific binding to the PBR of the two ligands. There may be other factors that contribute to the overall in vivo kinetics and binding of PBR radioligands. Hence,

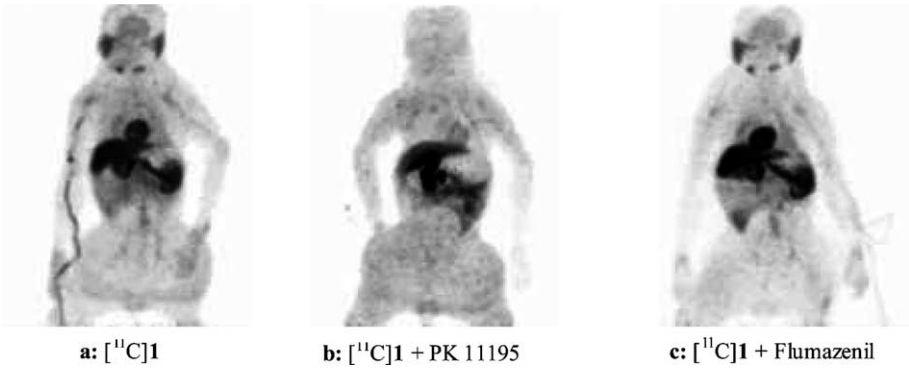

Figure 3. PET images of the body 1 h after iv injection of (a) [^{11}C]**1** (baseline), (b) [^{11}C]**1** + PK 11195 (5 mg/kg) and (c) [^{11}C]**1** + flumazenil (1 mg/kg).

more extensive studies are required to gain further insight into the PBR and its interaction with various ligands. This will ultimately lead to the design and synthesis of superior PBR ligands.

3. Conclusion

In this study, the pyrazolopyrimidine **1** (DPA-713) was synthesised, radiolabelled with carbon-11 and evaluated in a baboon using PET. [^{11}C]**1** was prepared by O-alkylation of the phenolic derivative **6** with [^{11}C]CH_3I in reproducible yields and specific activity. The results from the PET imaging studies were consistent with retention of [^{11}C]**1** in the baboon brain due to specific binding to the PBR. We therefore believe that this radioligand may be useful in detecting changes in PBR density in disease states and warrants further investigation. Because it is the first PBR ligand from the pyrazolopyrimidine class to be radiolabelled, it may generate novel information on the structure and physiological roles of the PBR in vivo.

4. Experimental

4.1. General

4.1.1. Chemicals and TLCs. Chemicals were purchased from Aldrich and used with no further purification. PK 11195 and flumazenil were purchased from Tocris, UK. Melting points were performed in a sealed capillary using a Stuart Melting Point Apparatus SMP3 and are uncorrected. Column chromatography was performed with Merck silica gel 60 (230–400 mesh). Thin layer chromatography (TLC) was carried out using aluminium-backed plates pre-coated with silica gel (60 F_{254}) and was developed using UV fluorescence (254 nm and/or 365 nm).

4.1.2. Spectroscopies. Proton nuclear magnetic resonance (^{1}H NMR) spectra were recorded using a 300 MHz Varian Gemini instrument. Chemical shifts (δ) are reported in parts per million (ppm) downfield from internal tetramethylsilane (TMS). Multiplicities are reported as s (singlet), d (doublet), dd (doublet of doublets), m (multiplet) and the observed coupling constant (J). Mass spec was carried out on a Thermo Finnigan Polaris Q GCMS instrument.

4.2. Chemistry

4.2.1. 3-(4-Methoxy-phenyl)-3-oxo-propionitrile (3). A mixture of methyl-4-methoxybenzoate (30 g, 181 mmol) and sodium methoxide (9.75 g, 181 mmol) was heated at 80 °C under an argon atmosphere with continuous stirring until homogeneous. Acetonitrile (16.5 mL, 313 mmol) and chlorobenzene (19 mL) were added dropwise to the mixture. The reaction was heated at 90–100 °C for 24 h with continuous stirring. After the mixture was cooled to 0 °C and treated with ice water (50 mL) and diethyl ether (200 mL), it was shaken until the solid material dissolved. The aqueous layer was separated from the organic layer and acidified to pH 2 with dilute H_2SO_4. Following the addition of diethyl ether, the organic layer was extracted, dried over anhydrous Na_2SO_4 and evaporated to dryness. The resulting yellow solid was dissolved in $CHCl_3$ and washed with saturated $NaHCO_3$ aqueous solution (5×100 mL) to remove benzoic acid. The organic layer was dried over anhydrous Na_2SO_4 and evaporated to dryness. The solid was purified by washing with petroleum ether which yielded **3**[19,20] (5.16 g, 17%) as fine, light yellow crystals; mp: 132–137 °C; ^{1}H NMR ($CDCl_3$, 300 MHz) δ 3.89 (s, 3H, OCH_3), 4.03 (s, 2H, CH_2), 6.97 (d, $J = 9.0$ Hz, 2H, Ph), 7.90 (d, $J = 9.0$ Hz, 2H, Ph).

4.2.2. 3-Cyano-*N*,*N*-diethyl-4-(4-methoxy-phenyl)-4-oxo-butyramide (4). A mixture of **3**[19,20] (2.0 g, 11.4 mmol), *N*,*N*-diethylchloroacetamide (1.7 g, 11.4 mmol) and NaI (5.1 g, 34 mmol) were added to a solution of NaOH (0.5 g, 12.5 mmol) in 80% EtOH (80 mL) while being stirred continuously. The mixture was stirred at room temperature for 7 h and monitored by TLC. Once the reaction was complete, it was allowed to cool and was filtered to remove the inorganic material. The filtrate was concentrated and the residue was purified by column chromatography (CH_2Cl_2 as eluent) to yield **4**[18] (2.1 g, 64%) as a dark yellow oil; ^{1}H NMR ($CDCl_3$, 300 MHz) δ 1.06–1.30 (m, 6H, $N(CH_2CH_3)_2$), 2.85 (dd, $J = 4.5$, 16.2 Hz, 1H, CH_2), 3.21–3.43 (m, 5H: 4H, $N(CH_2CH_3)_2$: 1H, CH_2), 3.90 (s, 3H, OCH_3), 4.89–5.02 (m, 1H, CH), 6.98 (d, $J = 8.7$ Hz, 2H, Ph), 8.05 (d, $J = 9.0$ Hz, 2H, Ph). Mass Spectrum: CI, m/z 289 (M + 1).

4.2.3. 2-[3-Amino-5-(4-methoxy-phenyl)-1*H*-pyrazol-4-yl]-*N*,*N*-diethylacetamide (5). Hydrazine hydrate (0.73 g, 14.6 mmol) and acetic acid (0.73 mL) were added to a solution of **4**[18] (2.1 g, 7.3 mmol) in EtOH (37 mL). The mixture was heated at reflux for 4 h and monitored by TLC. Once the reaction was complete, it was allowed to cool to room temperature. The solution was evaporated to dryness and the residue was purified by silica gel column chromatography (CH_2Cl_2/MeOH, 10:1 (v/v), as eluent). The purified product was re-dissolved in CH_2Cl_2 and washed with saturated $NaHCO_3$ aqueous solution (4×20 mL) to remove acetic acid. This afforded **5**[18] (1.52 g, 68%) as yellow crystals; mp: 154.5–157.5 °C; ^{1}H NMR ($CDCl_3$, 300 MHz) δ 0.90–1.10 (m, 6H, $N(CH_2CH_3)_2$), 3.04–3.33 (m, 4H, $N(CH_2CH_3)_2$), 3.50 (s, 2H, CH_2), 3.85 (s, 3H, OCH_3), 6.98 (d, $J = 8.7$ Hz, 2H, Ph), 7.32 (d, $J = 9.0$ Hz, 2H, Ph).

4.2.4. *N*,*N*-Diethyl-2-[2-(4-methoxy-phenyl)-5,7-dimethylpyrazolo[1,5-*a*]pyrimidin-3-yl]-acetamide (1). 2,4-Pentanedione (0.4 g, 4 mmol) was added to a solution of **5**[18] (1.2 g, 4 mmol) in EtOH (20 mL). The mixture was heated at reflux for 12 h. The reaction mixture was allowed to cool and the solvent was evaporated to dryness. The residue was purified by silica gel column chromatography ($CHCl_3$/MeOH, 40:1 (v/v), as eluent) which yielded **1**[18] (1.37 g, 93%) as pale yellow crystals; mp: 120.5–123.5 °C; ^{1}H NMR ($CDCl_3$, 300 MHz) δ 1.09–1.22 (m, 6H, $N(CH_2CH_3)_2$), 2.54 (s, 3H, 5-CH_3), 2.74 (s, 3H, 7-CH_3), 3.39–3.51 (m, 4H, $N(CH_2CH_3)_2$), 3.85 (s, 3H, OCH_3), 3.91 (s, 2H, CH_2), 6.51 (s, 1H, H-6), 6.98 (d, $J = 9.0$ Hz, 2 H, Ph), 7.76 (d, $J = 9.0$ Hz, 2H, Ph).

4.2.5. *N*,*N*-Diethyl-2-[2-(4-hydroxy-phenyl)-5,7-dimethyl-pyrazolo[1,5-*a*]pyrimidin-3-yl]-acetamide (6). A solution of **1**[18] (0.43 g, 1.16 mmol), hexadecyl tributyl phosphonium bromide (0.06 g, 0.116 mmol) and 45% HBr (6 mL) was heated at 100 °C for 7 h under constant stirring. The reaction mixture was basified to pH 8–9 using $NaHCO_3$ and extracted with CH_2Cl_2. The organic layer was collected and dried over anhydrous Na_2SO_4. The solvent was removed under vacuum and the residue was purified by column chromatography ($CHCl_3$/MeOH, 40:1 (v/v), as eluent) to yield **6** (220 mg, 54%) as ivory crystals; mp: 242.5–247 °C; ^{1}H NMR ($CDCl_3$, 300 MHz) δ 1.06–1.18 (m, 6H, $N(CH_2CH_3)_2$), 2.54 (s, 3H, 5-CH_3), 2.73 (s, 3H, 7-CH_3), 3.34–3.51 (m, 4H, $N(CH_2CH_3)_2$), 3.96 (s, 2H, CH_2), 6.49 (s, 1H, H-6), 6.79–6.82 (d, $J = 8.7$ Hz, 2H, Ph), 7.61–7.64 (d, $J = 8.4$ Hz, 2H, Ph); (Found, C, 66.35; H, 6.71; N, 15.38. $C_{20}H_{24}N_4O_2 \cdot 1/2H_2O$ requires C, 66.48; H, 6.93; N, 15.51%). Mass Spectrum: CI, *m*/*z* 353 (M + 1).

4.3. Radiochemistry

4.3.1. Preparation of [^{11}C]CH_3I. The target gas ($^{14}N + 0.5\%$ $^{16}O_2$) was bombarded with protons using a 16 MeV cyclotron to produce [^{11}C]CO_2. The [^{11}C]CO_2 was transferred to a GE Microlab automated module and concentrated onto molecular sieves. The sieves were heated to release [^{11}C]CO_2 which was reduced by hydrogen on a nickel catalyst to form [^{11}C]CH_4. The [^{11}C]CH_4 was released into the CH_3I conversion part of the module where it was recirculated through a quartz column (packed with ascarite and iodine crystals) by helium carrier gas. The [^{11}C]CH_3I formed was trapped in ascarite while any unconverted [^{11}C]CH_4 was transferred to waste.

4.3.2. Preparation and formulation of *N*,*N*-diethyl-2-[2-(4-[^{11}C]methoxy-phenyl)-5,7-dimethyl-pyrazolo[1,5-*a*]pyrimidin-3-yl]-acetamide, ([^{11}C]1). Under helium gas flow, the synthesised [^{11}C]CH_3I was delivered to a 1 mL reaction vessel containing **6** (0.5 mg, 0.0014 mmol) in DMF (300 μL) and tetrabutylammonium hydroxide (2 μL) and allowed to stand at room temperature for 3 min. The reaction mixture was diluted with 0.5 mL of a solution of 0.1 M NaH_2PO_4–CH_3CN (70:30, v/v) and injected onto a HPLC XTerra RP C-18 (100 × 7.8 mm, 5 μm) semi-preparative reverse-phase column. Using a mobile phase of 0.1 M NaH_2PO_4–CH_3CN (70:30, v/v) and a flow rate of 6.0 mL/min, the retention time (t_R) of [^{11}C]**1** was 6.5 min. The radioactive fraction corresponding to [^{11}C]**1** was collected and evaporated under vacuum. The residue was reconstituted in sterile saline (2 mL) and filtered through a sterile Millipore GS 0.22-μm filter into a sterile pyrogen free evacuated vial.

4.3.3. Quality control of [^{11}C]1. For determination of specific radioactivity and radiochemical purity, an aliquot of the final solution of known volume and radioactivity was injected onto an analytical reverse-phase HPLC column (XTerra RP C-18, 150 × 4.6 mm). A mobile phase of 0.1 M NaH_2PO_4–CH_3CN (50:50, v/v) at a flow rate of 1.0 mL/min was used to elute [^{11}C]**1** ($t_R = 2.3$ min). The area of the UV absorbance peak measured at 254 nm corresponding to the carrier product was measured (integrated) on the HPLC chromatogram and compared to a standard curve relating mass to UV absorbance.

4.4. PET studies

4.4.1. Animals. A male *Papio hamadryas* baboon aged 13 and weighing 26.5 kg was selected for PET scanning. The baboon was maintained and handled in accordance with the NHMRC code of practice for the care and use of non-human primates for scientific purposes. The project application was approved by the Central Sydney Area Health Service (CSAHS) Animal Ethics Committee.

4.4.2. Baboon PET imaging. All PET data were acquired using a Siemens Biograph LSO PET-CT scanner in the Department of PET and Nuclear Medicine at Royal Prince Alfred Hospital. This dual modality device has a fully 3D PET scanner with 24 crystal rings and a dual slice CT scanner in the same gantry. It yields a reconstructed PET spatial resolution of 6.3 mm FWHM (full width at half maximum) at the centre of the field of view. A CT scan of the head was completed prior to radioligand injection. The baboon was initially anaesthetised with ketamine (4 mg/kg, im) in addition to medetomidine hydrochloride (Domitor, 30 μg/kg, im) which is an α_2-adrenoceptor agonist. Anaesthesia was maintained with the use of an iv infusion of ketamine in saline at a dose rate of 0.2 mg ketamine/kg/min. The baboon also received $MgSO_4$ (2 mL) given over half an hour and atropine (1 mg) plus maxolon (5 mg). The head of the baboon was immobilized with plastic tape to minimise motion artefacts. Acquisition of dynamic PET data (20 × 30 s, 30 × 60 s and 4 × 300 s frames) was commenced just prior to radioligand injection and yielded a total of 54 frames over a period of 60 min.

The dynamic 3D PET data were rebinned using FORE (Fourier rebinning) and reconstructed into 47 transaxial slices with filtered backprojection and CT data based corrections for photon attenuation and scatter. Reconstructed voxel dimensions were 0.206 × 0.206 × 0.337 cm. The radioligand uptake was converted to units of percent injected dose per volume of brain tissue (% dose/mL) and plotted against time. An automated 3D registration algorithm[24] was used to co-register the three reconstructed scans prior to ROI definition. Decay corrected time–activity curves representing the variation in radioligand concentration versus time were constructed from selected slices for regions of interest over the whole brain.

After dynamic acquisition, a whole body PET-CT scan was performed to determine other sites of uptake of the radioligand.

4.4.3. Blocking studies. Both PK 11195 (5 mg/kg) and flumazenil (1 mg/kg) were dissolved in saline with a small quantity of propylene glycol and acetic acid. Both blocking drugs were injected intravenously 5 min prior to tracer injection into the cephalic vein. Drug treatments were separated by at least 3-week intervals.

4.5. Lipophilicity measurements

The $\log P_{7.4}$ was calculated (for derivative **1** and PK 11195) by employing a HPLC method previously described.[25] Phosphate buffer (0.1 M) was prepared by dissolving weighed amounts of potassium dihydrogen orthophosphate in HPLC water and the pH was adjusted to 7.5 with sodium hydroxide solution (0.1 M). Samples were analysed using a C-18 column (XTerra, 150×4.6 mm, 5 μm) and a mobile phase of MeOH and phosphate buffer (60:40 (v/v), pH 7.4) with a flow rate of 1 mL/min. The lipophilicity of each compound was estimated by comparing its retention time to that of standards having known $\log P$ values. The standards used to generate a general calibration equation were aniline, benzene, bromobenzene, ethyl benzene, trimethyl benzene and hexachlorobenzene dissolved in mobile phase. All sample injections were performed three times and the results were averaged to yield the final values. A calibration curve of $\log P$ versus retention time was produced which resulted in an experimental calibration equation ($y = 1.0791\ e^{0.7527x}$) with r^2 of 0.995. The exponential equation of the trendline function from the calibration graph and Excel™ allowed the $\log P$ values to be calculated.

Acknowledgments

The authors thank Ms. Jodie Brackenreg for technical assistance during imaging studies and Dr. Ken Mewett from the Adrien Albert Laboratory of Medicinal Chemistry for helpful discussions. This work was supported by DEST and the French Embassy in Australia under the FAST programme (FR040051).

References and notes

1. Braestrup, C.; Squires, R. F. *Proc. Natl. Acad. Sci. U.S.A.* **1977**, *74*, 3805.
2. Casellas, P.; Galiegue, S.; Basile, A. S. *Neurochem. Int.* **2002**, *40*, 475.
3. Gavish, M.; Bachmann, I.; Shoukrun, B.; Katz, Y.; Veenman, L.; Weisinger, G.; Weizman, A. *Pharmacol. Rev.* **1999**, *51*, 629.
4. Zavala, F. *Pharmacol. Ther.* **1997**, *75*, 199.
5. Taketani, S.; Kohno, H.; Furukawa, T.; Tokunaga, R. *J. Biochem. (Tokyo)* **1995**, *117*, 875.
6. Chelli, B.; Lena, A.; Vana Core, R.; Pozzo, E. D.; Costa, B.; Rossi, L.; Salvetti, A.; Scatena, F.; Ceruti, S.; Abbracchio, M. P.; Gremigni, V.; Martini, C. *Biochem. Pharmacol.* **2004**, *68*, 125.
7. Belloli, S.; Moresco, R. M.; Matrarres, M.; Biella, G.; Sanvito, F.; Simonelli, P.; Turolla, E.; Olivieri, S.; Capelli, A.; Vomera, S.; Galli-kienle, M.; Fazio, F. *Neurochem. Int.* **2004**, *44*, 433.
8. Galiegue, S.; Tinel, N.; Casellas, P. *Curr. Med. Chem.* **2003**, *10*, 1563.
9. Banati, R. B. *Glia* **2002**, *40*, 206.
10. Gonzalez-Scarano, F.; Baltuch, G. *Annu. Rev. Neurosci.* **1999**, *22*, 219.
11. Versijpt, J. J.; Dumont, F.; Van Laere, K. J.; Decoo, D.; Santens, P.; Audenaert, K.; Achten, E.; Slegers, G.; Dierchx, R. A.; Korf, J. *Eur. Neurol.* **2003**, *50*, 39.
12. Bribes, E.; Carriere, D.; Goubet, C.; Galiegue, S.; Casellas, P.; Simony-Lafontaine, J. *J. Histochem. Cytochem.* **2004**, *52*, 19.
13. Cagnin, A.; Brooks, D. J.; Kennedy, A. M.; Gunn, R. N.; Myers, R.; Turkheimer, F. E.; Jones, T.; Banati, R. B. *Lancet* **2001**, *358*, 461.
14. Banati, R. B.; Newcombe, J.; Gunn, R. N.; Cagnin, A.; Turkheimer, F.; Heppner, F.; Price, G.; Wegner, F.; Giovannoni, G.; Miller, D. H.; Perkin, G. D.; Smith, T.; Hewson, A. K.; Bydder, G.; Kreutzberg, G. W.; Jones, T.; Cuzner, M. L.; Myers, R. *Brain* **2000**, *123*, 2321.
15. Gerhard, A.; Banati, R. B.; Goerres, G. B.; Cabnin, A.; Myers, R.; Gunn, R. N.; Turkheimer, F.; Good, C. D.; Mathias, C. J.; Quinn, N.; Schwarz, J.; Brooks, D. J. *Neurology* **2003**, *61*, 686.
16. Zhang, M.; Kida, T.; Noguchi, J.; Furutsuka, K.; Maeda, J.; Suhara, T.; Suzuki, K. *Nucl. Med. Biol.* **2003**, *30*, 513.
17. Maeda, J.; Suhara, T.; Zhang, M.; Okauchi, T.; Yasuno, F.; Ikoma, Y.; Inaji, M.; Nagai, Y.; Takano, A.; Obayashi, S.; Suzuki, K. *Synapse* **2004**, *52*, 283.
18. Selleri, S.; Bruni, F.; Costagli, C.; Costanzo, A.; Guerrini, G.; Ciciani, G.; Costa, B.; Martini, C. *Bioorg. Med. Chem.* **2001**, *9*, 2661.
19. Dorsch, J. B.; McElvain, S. M. *J. Am. Chem. Soc.* **1932**, *54*, 2960.
20. Long, R. S. *J. Am. Chem. Soc.* **1947**, *69*, 990.
21. Petit-Taboue, M.; Baron, J.; Barre, L.; Travere, J.; Speckle, D.; Camsonne, R.; Mackenzie, E. *Eur. J. Pharmacol.* **1991**, *200*, 347.
22. Lockhart, A.; Davis, B.; Matthews, J. C.; Rahmoune, H.; Hong, G.; Gee, A.; Earnshaw, D.; Brown, J. *Nucl. Med. Biol.* **2003**, *30*, 199.
23. Halldin, C.; Gulyas, B.; Langer, O.; Farde, L. *Q. J. Nucl. Med.* **2001**, *45*, 139.
24. Eberl, S.; Kanno, F.; Fulton, R. R.; Ryan, A.; Hutton, B. F.; Fulham, M. J. *J. Nucl. Med.* **1996**, *37*, 137.
25. Quinlivan, M.; Mattner, F.; Papazian, V.; Zhou, J.; Katsifis, A.; Emond, P.; Chalon, S.; Kozikowski, A.; Guilloteau, D.; Kassiou, M. *Nucl. Med. Biol.* **2003**, *30*, 741.